

ELECTROCATALYTIC OXIDATION OF METHANOL BY THE $[\text{Ru}_3\text{O}(\text{OAc})_6(\text{py})_2(\text{CH}_3\text{OH})]^{3+}$ CLUSTER: IMPROVING THE METAL-LIGAND ELECTRON TRANSFER BY ACCESSING THE HIGHER OXIDATION STATES OF A MULTICENTERED SYSTEM*

Henrique E. Toma* e Koiti Araki

Instituto de Química, Universidade de São Paulo, CP 26077, 05513-970 São Paulo - SP, Brasil

André Luiz Barboza Formiga

Instituto de Química, Universidade Estadual de Campinas, CP 6154, 13084-971 Campinas - SP, Brasil

Anamaria D. P. Alexiou

Universidade Presbiteriana Mackenzie, R. da Consolação, 896, 01302-907 São Paulo - SP, Brasil

Genebaldo S. Nunes

Universidade Estadual do Sudoeste da Bahia, Pç. Primavera, 40, 45700-000 Itapetinga - BA, Brasil

Recebido em 24/5/10; aceito em 27/7/10; publicado na web em 15/10/10

The $[\text{Ru}_3\text{O}(\text{OAc})_6(\text{py})_2(\text{CH}_3\text{OH})]^+$ cluster provides an effective electrocatalytic species for the oxidation of methanol under mild conditions. This complex exhibits characteristic electrochemical waves at -1.02, 0.15 and 1.18 V, associated with the $\text{Ru}_3^{\text{III,III,III}}/\text{Ru}_3^{\text{III,III,III}}/\text{Ru}_3^{\text{IV,III,III}}$ successive redox couples, respectively. Above 1.7 V, formation of two Ru^{IV} centers enhances the 2-electron oxidation of the methanol ligand yielding formaldehyde, in agreement with the theoretical evolution of the HOMO levels as a function of the oxidation states. This work illustrates an important strategy to improve the efficiency of the oxidation catalysis, by using a multicentered redox catalyst and accessing its multiple higher oxidation states.

Keywords: ruthenium-acetate clusters; methanol oxidation; electrocatalysis.

INTRODUCTION

Electrochemical oxidation of organic compounds is an important issue in modern technology, allowing, for instance, the rational use of biomass as chemical supply and also in clean energy conversion processes.¹ In this sense, the development of new electrocatalysts based on transition metal complexes has been pursued with great interest, because of their wide range of redox potentials, and variety of active centers in association with low reorganization barriers for electron transfer.²⁻⁵ A typical case of efficient transition metal electrocatalysis has been reported for the oxidation of 4-substituted-1,2-dimethoxybenzenes, in the presence of iron(II)polyimine catalysts.⁶

In this regard, we have investigated the catalytic properties of ruthenium carboxylate clusters of the type $[\text{Ru}_3\text{O}(\text{OAc})_6(\text{py})_2\text{L}]^{n+}$ in the oxidation of organic compounds^{7,8} ($\text{OAc} = \text{CH}_3\text{CO}_2^-$, $\text{py} = \text{pyridine}$). These clusters exhibit a triangular structure strongly held by a central μ -oxo bridge, as well as by three double carboxylate bridges^{9,10} as shown in Figure 1. The close proximity of the metal centers leads to substantial metal-metal coupling, enhancing the electronic delocalization in the triangular unit.

Drago *et al.*^{11,12} have reported on the catalytic oxidation of primary alcohols to aldehydes and of secondary alcohols to ketone by $[\text{Ru}_3\text{O}(\text{O}_2\text{CR})_3\text{L}_3]^{n+}$ complexes ($\text{R} = \text{CH}_3, \text{C}_2\text{H}_5; \text{L} = \text{H}_2\text{O}, \text{PPh}_3$). The catalysis was carried out at 65 °C under 40 psi of O_2 during 12-24 h. Recently, we have shown^{7,8} that a particularly efficient catalyst in oxygen transfer reactions under mild conditions is the oxo-bridged ruthenium carboxylate cluster $[\text{Ru}_3\text{O}(\text{OAc})_6(\text{py})_2(\text{O})]^+$ (Figure 1b). This species can be represented as $[\text{Ru}_3^{\text{IV,IV,III}}=\text{O}]$, and is rather special, since it exhibits two Ru^{IV} centers for activating the $\text{Ru}=\text{O}$ bond in oxygen transfer reactions. As a matter of fact, it exhibits excellent

catalytic activity in the oxidation of benzyl alcohol to benzyl aldehyde, and even in the catalytic oxidation of hydrocarbons. A convenient way of obtaining this species is from the $[\text{Ru}_3\text{O}(\text{OAc})_6(\text{py})_2(\text{H}_2\text{O})]^+$ cluster by means of proton-coupled redox processes, or by activating $[\text{Ru}_3\text{O}(\text{OAc})_6(\text{py})_2(\text{X})]^+$ species, where $\text{X} = \text{CH}_3\text{OH}$ or DMSO , using oxygen donors such as iodosylbenzene or *tert*-butylhydroperoxide. In the last case, it should be noticed that a high catalytic activity is only observed in the presence of ligands such as CH_3OH or $(\text{CH}_3)_2\text{SO}$ which are easily oxidized, yielding, respectively, the weakly-coordinating formaldehyde or $(\text{CH}_3)_2\text{SO}_2$ species. Formation of such leaving groups greatly facilitates the oxygen transfer from the incoming oxidizing agent.

In this work, we explored a different catalytic route for the $[\text{Ru}_3\text{O}(\text{OAc})_6(\text{py})_2\text{L}]^{n+}$ complexes, by focusing on the methanol derivative (Figure 1c). In contrast to the preceding examples which require oxygen donor species, such as iodosyl benzene and peroxides to promote the catalysis, here we pursued the direct electrocatalytic oxidation of methanol by the cluster species. As a matter of fact, the $[\text{Ru}_3\text{O}(\text{OAc})_6(\text{py})_2(\text{CH}_3\text{OH})]^+$ complex can be viewed as an interesting candidate for the electrochemical oxidation of methanol, because of its favorable electron transfer characteristics, and of the ability of the ruthenium clusters to stabilize high oxidation potentials, *via* the multicentered system, increasing the possibilities of performing multielectron transfer processes. In this way, it is expected that the $[\text{Ru}_3\text{O}(\text{OAc})_6(\text{py})_2(\text{CH}_3\text{OH})]^{n+}$ cluster at high oxidation states, e.g. $\text{Ru}^{\text{IV,IV,III}}$, can oxidize the coordinated methanol ligand, generating a leaving group for the access of another methanol molecule from the solvent in order to accomplish the catalytic cycle.

Along this line, we started investigating the electrochemical and spectroelectrochemical behavior of the $[\text{Ru}_3\text{O}(\text{OAc})_6(\text{py})_2(\text{CH}_3\text{OH})]^+$ complex (Figure 1c), or $[\text{Ru}_3^{\text{III,III,III}}(\text{CH}_3\text{OH})]^+$, aiming the exploitation of its multiple oxidation states in the electrocatalytic oxidation of methanol under mild conditions. It should be noticed that the electro-

*e-mail: henetoma@iq.usp.br

*Dedicated to Prof. Hans Viertler, by the occasion of his 70th anniversary.

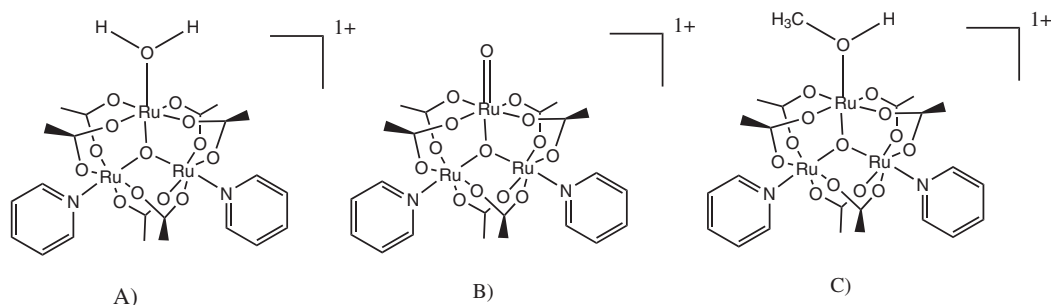


Figure 1. Structural formula of the $[\text{Ru}_3\text{O}(\text{OAc})_6(\text{py})_2\text{L}]^+$ clusters: a) $\text{L} = \text{H}_2\text{O}$; b) $\text{L} = \text{O}$; c) $\text{L} = \text{CH}_3\text{OH}$

catalytic oxidation of methanol is a very important issue, in energy conversion, including fuel cells. Recently, a large number of papers dealing the with electrocatalytic oxidation of methanol have been published; focusing mostly on modified electrodes encompassing metal oxides, carbon nanotubes and molecular species.¹³⁻²²

EXPERIMENTAL

Materials and instrumentation

Analytical grade reagents and solvents (Aldrich or Merck) were used as supplied. Deionized water was obtained with a Barnstead nanopure purification system. Sodium trifluoroacetate (NaTFA) and its methanolic solutions were kept dry in the presence of 3 Å molecular sieves. Tetraethylammonium perchlorate (TEAClO_4) was prepared according to procedures previously described.²³

$[\text{Ru}_3\text{O}(\text{OAc})_6(\text{py})_2(\text{CH}_3\text{OH})]\text{PF}_6$ was prepared by adapting the four steps procedure previously reported in the literature.²⁴ The initial step involves the synthesis of the $[\text{Ru}_3\text{O}(\text{OAc})_6(\text{CH}_3\text{OH})_3]\text{OAc}$ complex from the reaction of $\text{RuCl}_3 \cdot n\text{H}_2\text{O}$ with $\text{NaOAc} \cdot 3\text{H}_2\text{O}$. Typically, 5.0 of $\text{RuCl}_3 \cdot n\text{H}_2\text{O}$ were dissolved in a mixture of 120 mL of dry ethanol and 28 mL of acetic acid in a round bottomed flask (500 mL) and 10.2 g of $\text{NaOAc} \cdot 3\text{H}_2\text{O}$ were added in small portions. The mixture was kept under reflux for 4 h and allowed to under rest overnight. The solid residues containing NaOAc and NaCl were removed by filtration, and the cluster solution was evaporated to dryness in a flash evaporator. The oily material was treated with 100 mL of methanol, and evaporated to dryness. This procedure was repeated for three times. Then 200 mL of acetone was added, yielding a green precipitate of $[\text{Ru}_3\text{O}(\text{OAc})_6(\text{CH}_3\text{OH})_3]\text{OAc}$ which was collected on a filter, and washed with diethyl ether. In a second step, the $[\text{Ru}_3\text{O}(\text{OAc})_6(\text{CH}_3\text{OH})_3]\text{OAc}$ complex was converted into the tris-substituted pyridine derivative, in the reduced form, $[\text{Ru}_3\text{O}(\text{OAc})_6(\text{py})_3]$. For this purpose, the previously obtained solid (6.0 g) was dissolved into 350 mL of methanol containing 27 mL of pyridine. The mixture was kept under reflux for 5 min. After cooling at room temperature, the mixture was transferred to an ice bath and 30 mL of hydrazine solution (51%) was gradually added, under stirring. After 15 min the precipitate of $[\text{Ru}_3\text{O}(\text{OAc})_6(\text{py})_3]$ was collected on a filter, and washed with small amounts of water, methanol and diethyl ether. In the third step, the $[\text{Ru}_3\text{O}(\text{OAc})_6(\text{py})_3]$ complex was treated with of CO to yield $[\text{Ru}_3\text{O}(\text{OAc})_6(\text{CO})(\text{py})_2]$. Accordingly, the $[\text{Ru}_3\text{O}(\text{OAc})_6(\text{py})_3]$ complex (4.0 g) was dissolved in a mixture of 90 mL of methanol and 270 mL of benzene, under an argon atmosphere. The mixture was kept under reflux in the presence of CO (generated from sulfuric acid and formic acid) which was bubbled into the solution for at least 5 h. After cooling, the blue complex $[\text{Ru}_3\text{O}(\text{OAc})_6(\text{CO})(\text{py})_2] \cdot \text{C}_6\text{H}_6$ precipitated. The solid was collected on a filter, and washed with diethyl ether. In the final step this complex was oxidized with bromine in the presence of NH_4PF_6 ,

to yield the $[\text{Ru}_3\text{O}(\text{OAc})_6(\text{py})_2(\text{CH}_3\text{OH})]\text{PF}_6$ product. In this way, the $[\text{Ru}_3\text{O}(\text{OAc})_6(\text{CO})(\text{py})_2] \cdot \text{C}_6\text{H}_6$ complex (3.3 g) was dissolved in 330 mL of CH_2Cl_2 and treated, under stirring, with 65 mL of a Br_2 (0.15 mol L^{-1}) solution in CH_2Cl_2 . The solution was evaporated to dryness, and the solid residue dissolved in 250 mL of methanol. The solution was kept under reflux for 30 min and then 3.5 g of NH_4PF_6 dissolved in 20 mL of methanol was added. After cooling, the $[\text{Ru}_3\text{O}(\text{OAc})_6(\text{py})_2(\text{CH}_3\text{OH})]\text{PF}_6$ complex precipitated (3.2 g) as a blue solid and was collected on a filter and washed with diethyl ether. Anal. $\text{C}_{23}\text{H}_{32}\text{O}_{14}\text{N}_2\text{PF}_6\text{Ru}_3$ (experimental/calculated) for C 27.0/27.4; H 3.2/3.2; N 2.9/2.8 (net yield = 42%).

The electronic spectra were obtained with a Hewlett-Packard model 8453-A diode-array spectrophotometer. Cyclic voltammetry experiments were carried out using a potentiostat/galvanostat PGS-TAT 30 from Autolab and conventional three-electrode cell constituted by a vitreous carbon working electrode ($A = 0.025 \text{ cm}^2$); a platinum wire auxiliary electrode and an Ag/AgNO_3 (0.01 mol dm^{-3} ; $E^0 = 0.503 \text{ V vs SHE}$) reference electrodes. A three-electrode system, arranged in a rectangular quartz cell ($l = 0.25 \text{ mm}$) was used for the spectroelectrochemical measurements. In this case, a gold minigrad was used as a transparent working electrode, with the above mentioned auxiliary and reference minielectrodes.

Theoretical calculations

The geometries of $[\text{Ru}_3\text{O}(\text{OAc})_6(\text{py})_2\text{L}_3]^n$ ($\text{L} = \text{CH}_3\text{OH}$, $n = 0-3$), CH_2O and CH_3OH were optimized using a modified MM2 force field²⁵ with charges calculated by the semiempirical ZINDO/S method²⁶ as implemented in the HyperChem program using the same methodology previously reported.²⁷ A conjugate gradient with a $10^{-3} \text{ kcal mol}^{-1} \text{ \AA}^{-1}$ convergence limit were used for geometries. ZINDO/S Self-Consistent Field calculations were performed to obtain RHF wavefunctions with a $10^{-7} \text{ kcal mol}^{-1}$ criterion for convergence. For the species with half-integral spin states, the half-electron technique of Pople was used.²⁸

RESULTS AND DISCUSSION

Cyclic voltammetry

The cyclic voltammograms of the $[\text{Ru}_3\text{O}(\text{CH}_3\text{COO})_6(\text{py})_2(\text{CH}_3\text{OH})]^+$ cluster in methanol (Figure 2) exhibited three characteristic waves in the range of potentials from -1.50 to 1.50 V vs. SHE (Table 1) ascribed to the $\text{Ru}_3^{\text{III,III,II}}/\text{Ru}_3^{\text{III,III,III}}/\text{Ru}_3^{\text{III,III,III}}/\text{Ru}_3^{\text{IV,III,III}}$ successive redox couples.⁷ In particular, the $\text{Ru}_3^{\text{III,III,III}}/\text{Ru}_3^{\text{III,III,II}}$ ($E_{1/2} = -1.02 \text{ V vs. SHE}$) and $\text{Ru}_3^{\text{III,III,III}}/\text{Ru}_3^{\text{III,III,III}}$ ($E_{1/2} = 0.15 \text{ V vs. SHE}$) couples exhibited reversible behavior ($i_p/i_{p_c} \sim 1$, $\Delta E = 59-60 \text{ mV}$), while the $\text{Ru}_3^{\text{IV,III,III}}/\text{Ru}_3^{\text{III,III,III}}$ ($E_{1/2} = 1.18 \text{ V vs. SHE}$) process was quasi-reversible ($i_p/i_{p_c} \sim 1$, $\Delta E = 80 \text{ mV}$), showing some influence of a coupled chemical reaction, but at a very small extent. It should be noticed that the $\text{Ru}_3^{\text{IV,III,III}}$ species

is a relatively strong oxidizing agent, capable of oxidizing methanol to formaldehyde ($E^0 = 0.19$ V).²⁹ This reaction may be contributing to the broadening of the waves, however it should be relatively slow in the time scale of the cyclic voltammetry.

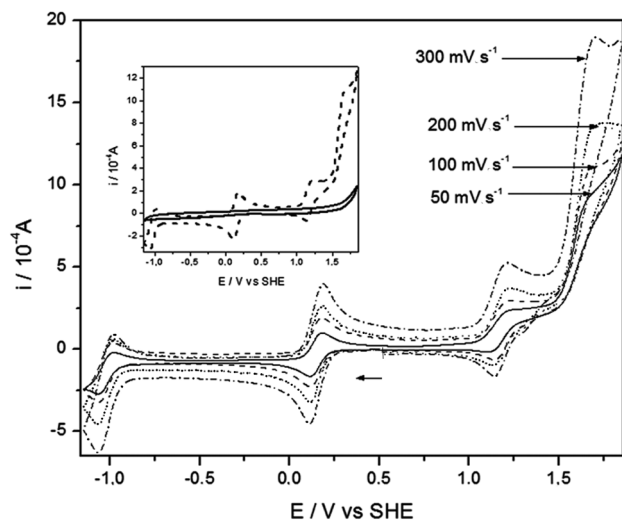


Figure 2. Cyclic voltammograms of a 5.0×10^{-3} mol dm^{-3} solution of $[\text{Ru}_3\text{O}(\text{Ac})_6(\text{py})_2(\text{CH}_3\text{OH})]^+$ in methanol, 0.10 mol dm^{-3} NaTFA, using a glassy carbon disc electrode; inset: cyclic voltammogram (scan rate = 50 mV s^{-1}) of methanol (base line) and of the ruthenium cluster, for comparison purposes

Table 1. Electrochemical data for the $[\text{Ru}_3\text{O}(\text{Ac})_6(\text{py})_2(\text{CH}_3\text{OH})]^+$ cluster in methanol^a

Redox couple	$E_{1/2}$ / mV	$\Delta E_{1/2}$ / mV
$\text{Ru}^{\text{III,III,III}}\text{MeOH}/\text{Ru}^{\text{III,III,III}}\text{MeOH}$	-1.02	59
$\text{Ru}^{\text{III,III,III}}\text{MeOH}/\text{Ru}^{\text{III,III,III}}\text{MeOH}$	0.15	60
$\text{Ru}^{\text{IV,III,III}}\text{MeOH}/\text{Ru}^{\text{III,III,III}}\text{MeOH}$	1.18	80
$\text{Ru}^{\text{IV,IV,III}}\text{MeOH}/\text{Ru}^{\text{IV,III,III}}\text{MeOH}^c$	1.7 ^c	-

^aPotentials vs SHE; ^b 0.1 mol dm^{-3} NaTFA, Ag/Ag⁺ reference electrode, glassy carbon working electrode; ^credox wave involving methanol oxidation as a coupled reaction

At 1.7 V, a very strong anodic wave can be observed in methanol solution, with practically no counterpart in the reverse scan. This wave is close to the region expected for the $\text{Ru}_3^{\text{IV,IV,III}}/\text{Ru}_3^{\text{IV,III,III}}$ redox process, but it is much more intense than expected for a single mono-electronic process. The observed enhancement and the lack of the cathodic counterpart are consistent with an electrochemical process followed by a fast chemical reaction.³⁰

Sundholm^{31,32} reported that the anodic oxidation of methanol involves an electron transfer mechanism coupled with the deprotonation of the molecule, i.e. Scheme 1:

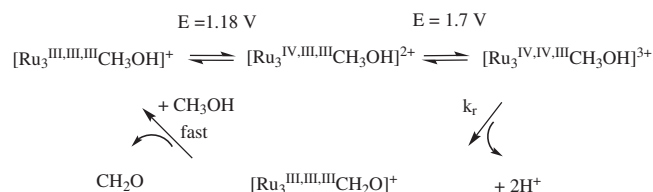


Scheme 1

The unstable CH_2OH^+ intermediate rapidly releases another proton, generating formaldehyde, CH_2O .

A similar reaction can be proposed for the oxidation of methanol coordinated to the ruthenium cluster species, $\text{Ru}^{\text{IV,IV,III}}$, at 1.7 V. Now, in addition to a higher redox potential in relation to the $\text{Ru}_3^{\text{IV,III,III}}$ species, the presence of two equivalent +IV oxidation states in the cluster species allows the extraction of two electrons from the coordinated methanol ligand (Scheme 1), generating formaldehyde,

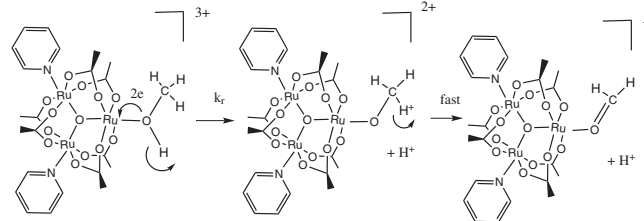
and the corresponding $\text{Ru}^{\text{III,III,III}}$ cluster. As a matter of fact, positive formaldehyde tests were observed using Nash method.³³ Therefore, the $\text{Ru}^{\text{IV,IV,III}}$ species should be a much better oxidizing agent than $\text{Ru}^{\text{IV,III,III}}$. On the other hand, according to a previous work^{3,4} formaldehyde is a labile ligand, and should dissociate very rapidly from the coordination sphere of the cluster, leaving space for entering another solvent molecule. In this way, the methanol complex is regenerated, completing the catalytic cycle shown in Scheme 2.



Scheme 2

This scheme resembles the type VII case theoretically described by Shain and Nicholson, for a catalytic reaction coupled to reversible charge transfer.²⁶ As a matter of fact, the observed voltammogram profiles above 1.5 V (Figure 2) are compatible with those theoretically predicted for this type of process. In this case, the current functions are usually expressed as a function of the k_f/a parameter, where k_f is the kinetic constant for the coupled chemical reaction and $a = Fv/RT$, where v = potential scan rate and the remaining terms have the conventional meaning. Based on such theoretical data, Shain and Nicholson³⁰ proposed a working curve in which the theoretical ratio of the catalytic peak current to the reversible peak current ($R = i_{\text{cat}}/i_{\text{rev}}$) is plotted as a function of $(k_f/a)^{1/2}$. From this plot, using the experimental values of R , it is possible to extract the value of k_f for the ruthenium cluster catalyst.

In our case, the reversible peak current can be estimated from the reversible voltammogram corresponding to the $\text{Ru}^{\text{III,III,III}}/\text{Ru}^{\text{IV,III,III}}$ process at 0.15 V. The catalytic peak currents were estimated from the voltammograms at 1.7 V, at the several scan rates, after subtracting the extrapolated base lines for the pure solvent. The values of $a^{1/2}$ calculated for the scan rates $v = 50, 100, 200$ and 300 mV s^{-1} were $1.39, 1.97, 2.78$ and 3.41 , respectively. The corresponding values of R were $5.5, 3.8, 3.3$ and 2.9 , respectively. By inserting such values into the Shain and Nicholson theoretical working curve,³⁰ the kinetic constant k_f were estimated as $12, 12, 15,$ and 18 s^{-1} , respectively, corresponding to an average value of 15 ± 3 s^{-1} . This result for k_f should reflect mainly the intramolecular electron transfer rate from the $\text{Ru}^{\text{IV,IV,III}}$ species to the coordinated methanol ligand, since the proton release from the intermediates to yield formaldehyde is expected to be very fast, as illustrated in the Scheme 3.



Scheme 3

It should be noted that the oxidation of the coordinated methanol ligand proceeds with a lifetime ($\tau = 1/k_f = 0.66$ s) concurrent with the time scale of the cyclic voltammetry, thus explaining why it exerts a dramatic influence on the shape and intensities of the electrochemical peaks at 1.7 V. In the case of a slower process, only a quasi-reversible electrochemical wave would be observed, similar to that at 1.18 V, where the catalyst exhibits only one Ru^{IV} site and is not strongly

oxidizing enough to perform a 2-electron oxidation of methanol. On the other hand, if k_f was extremely fast, the shape of the catalytic waves would tend to a limiting case, where the voltammograms converge into a plateau, in which the current becomes independent of the potential scan rates.

Spectroelectrochemistry

The electronic spectrum of the $[\text{Ru}_3\text{O}(\text{OAc})_6(\text{py})_2(\text{CH}_3\text{OH})]^+$ cluster in methanolic solution (Figure 3) exhibits a composite band at 678 nm ($\epsilon = 4030 \text{ mol}^{-1} \text{ cm}^{-1} \text{ L}$) ascribed to intracluster transitions in the $\text{Ru}_3^{\text{III,III,III}}$ species, in addition to a shoulder near 340 nm, which has been assigned to a $\text{Ru}_3\text{O}(\text{d}\pi) \rightarrow \text{py}(\pi^*)$ charge-transfer transition.¹⁰ UV-Vis spectroelectrochemical measurements in methanol can be seen in Figure 3. Starting from 0.5 V (vs. SHE) and going in the direction of more negative potentials (Figure 3a), one can observe a decrease of the bands at 678 nm, and an increase of two bands at 390 and 915 nm corresponding, respectively, to the $(\text{d}\pi) \rightarrow \text{py}(\pi^*)$ charge-transfer and the intracluster transitions in the reduced species $[\text{Ru}_3^{\text{III,III,II}}(\text{CH}_3\text{OH})]$.

It is important to note that by scanning the potential up to 1.8 V, there is no significant changes in the electronic spectra of the $[\text{Ru}_3^{\text{III,III,III}}(\text{CH}_3\text{OH})]^+$ species, in spite of the existence of two electrochemical waves in this region (Figures 2 and 3b). This observation is consistent with the proposed electrocatalytic process. In the time scale of the spectroelectrochemical measurements, the oxidized species cannot be detected since it is rapidly converted into formaldehyde, regenerating the starting $[\text{Ru}_3^{\text{III,III,III}}(\text{CH}_3\text{OH})]^+$ species absorbing at 678 nm.

Molecular modeling

Theoretical calculations were carried out to understand how the energy levels vary with the oxidations states of the $[\text{Ru}_3\text{O}(\text{OAc})_6(\text{py})_2(\text{CH}_3\text{OH})]^n$ clusters ($n = 0-3$), in relation to the HOMO levels of methanol. Initially the geometries of the clusters were optimized using a modified MM2 force field²⁵ and the charges calculated by the semiempirical ZINDO/S method.^{26,27} Then

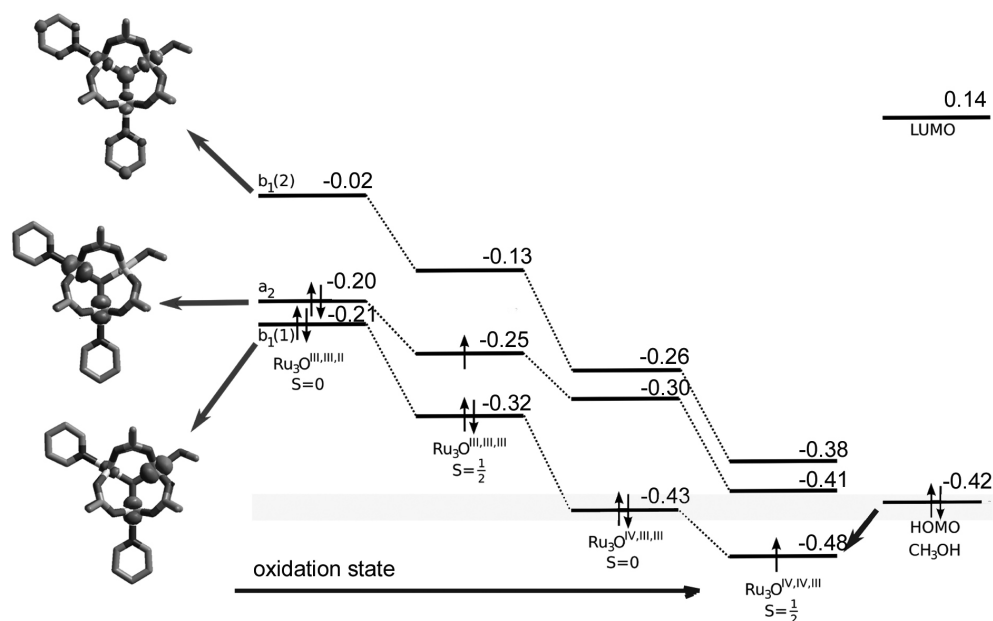


Figure 4. Representation of the HOMO levels (Hartree) for the $[\text{Ru}_3\text{O}(\text{OAc})_6(\text{py})_2(\text{CH}_3\text{OH})]^n$ clusters, and their energy dependence on the oxidation states, showing the crossover point for electron transfer, at the $\text{Ru}_3^{\text{IV,IV,III}}$ state

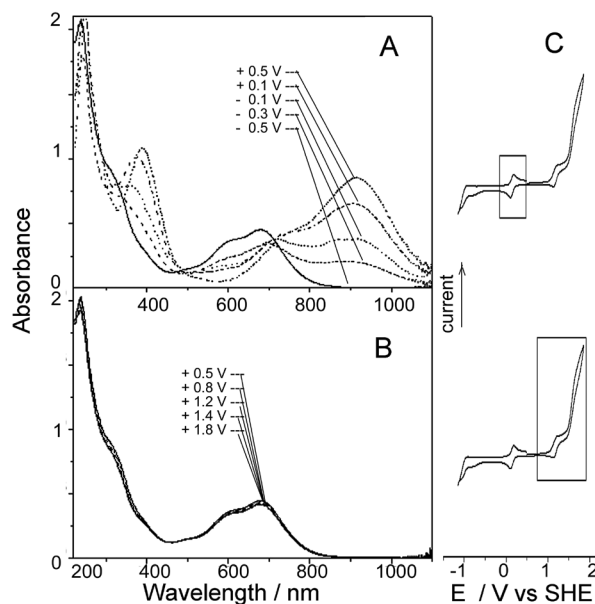


Figure 3. Spectroelectrochemistry of the $5.0 \times 10^{-3} \text{ mol dm}^{-3}$ solution of the $[\text{Ru}_3\text{O}(\text{OAc})_6(\text{py})_2(\text{CH}_3\text{OH})]\text{PF}_6$ cluster in methanol, 0.1 mol dm^{-3} NaTFA, from +0.5 to -0.5 V (a) and +0.5 to 1.8 V (b) in association with their corresponding ranges in the cyclic voltammograms (c)

ZINDO/S Self-Consistent Field calculations were performed to obtain RHF wavefunctions. For the species with half-integral spin states, the half-electron technique of Pople was used.²⁸ The results were collected in Figure 4.

As one can see in Figure 4, the three most relevant HOMO levels for the ruthenium clusters are centered on the Ru_3O core, exhibiting $b_1(1)$, a_2 and $b_1(2)$ symmetry. The b_1 levels exhibit a major contribution from the Ru atom coordinated to the methanol ligand. As the cluster oxidation states increase, there is a systematic decrease in the energies of the three HOMO levels. At the $\text{Ru}_3^{\text{IV,IV,III}}$ oxidation state, the cluster HOMO level (-0.43 Hartree) practically coincides with the methanol HOMO level (-0.42 Hartree), reaching the crossover

point for electron transfer. Moving down to the $\text{Ru}_3^{\text{IV,IV,III}}$ oxidation state, the HOMO level (-0.48 V) becomes far below the methanol HOMO level (-0.42), thus creating favorable conditions for electron transfer, as observed experimentally.

CONCLUSIONS

The electrochemistry of the $[\text{Ru}_3\text{O}(\text{Ac})_6(\text{py})_2(\text{CH}_3\text{OH})]^+$ cluster involves a series of reversible or quasi-reversible waves at -1.02, 0.15 and 1.18 V associated with the $\text{Ru}_3^{\text{III,III,II}}/\text{Ru}_3^{\text{III,III,II}}/\text{Ru}_3^{\text{III,III,III}}/\text{Ru}_3^{\text{IV,III,III}}$ successive redox couples, respectively. Above 1.5 V the oxidation of the $\text{Ru}_3^{\text{IV,III,III}}$ to the $\text{Ru}_3^{\text{IV,IV,III}}$ state is accompanied by the 2-electron oxidation of the coordinated methanol ligand, yielding formaldehyde and regenerating the $\text{Ru}_3^{\text{III,III,III}}$ species which returns to the cycle after incorporating another methanol ligand. Such reactions proceed at the time scale of the cyclic voltammograms. For this reason, at the slower time scale of the spectroelectrochemical experiments, only the $\text{Ru}_3^{\text{III,III,III}}$ species can be detected in the potential range of 0.5 to 1.8 V. The electrochemical responses at 1.18 and 1.7 V are consistent with the evolution trends of the HOMO levels with respect to the oxidation states, supporting the conclusion that at least two Ru^{IV} sites in the multicentered complex are required for an efficient electron transfer involving the oxidation of methanol. This relevant aspect should be taken into consideration in the design of more effective electrocatalytic species, capable of performing the oxidation of methanol under mild conditions.

ACKNOWLEDGEMENTS

The financial support from FAPESP, CNPq and CAPES is gratefully acknowledged.

REFERENCES

1. Viertler, H.; Gruber, J.; Pardini, V. L. In *Organic electrochemistry*; Lund, H.; Hammerich, O., eds.; Marcel Dekker: New York, 2001, chap. 17, p. 621.
2. Araki, K.; Toma, H. E. In *N-4 macrocyclic metal complexes*; Zagal, J. H.; Bedioui, F.; Dodelet, J.-P.; Springer: New York, 2006, chap. 6, p. 255.
3. Araki, K.; Dovidauskas, S.; Winnischofer, H.; Alexiou, A. D. P.; Toma, H. E.; *J. Electroanal. Chem.* **2001**, *498*, 152.
4. Dovidauskas, S.; Toma, H. E.; Araki, K.; Sacco, H. C.; Yamamoto, Y.; *Inorg. Chim. Acta* **2000**, *305*, 208.
5. Toma, H. E.; Araki, K.; *Progr. Inorg. Chem.* **2009**, *56*, 379.
6. Kuwabara, I. H.; Comminos, F. C. M.; Pardini, V. L.; Viertler, H.; Toma, H. E.; *Electrochim. Acta* **1994**, *39*, 2401.
7. Nunes, G. S.; Alexiou, A. D. P.; Araki, K.; Formiga, A. L. B.; Rocha, R. C.; Toma, H. E.; *Eur. J. Inorg. Chem.* **2006**, 1487.
8. Nunes, G. S.; Alexiou, A. D. P.; Toma, H. E.; *J. Catal.* **2008**, *260*, 188.
9. Alexiou, A. D. P.; Dovidauskas, S.; Toma, H. E.; *Quim. Nova* **2000**, *23*, 785.
10. Toma, H. E.; Araki, K.; Alexiou, A. D. P.; Nikolaou, S.; Dovidauskas, S.; *Coord. Chem. Rev.* **2001**, *219-221*, 187.
11. Davis, S.; Drago, R. S.; *Inorg. Chem.* **1988**, *27*, 4759.
12. Bilgrien, C.; Davis, S.; Drago, R. S.; *J. Am. Chem. Soc.* **1987**, *109*, 3786.
13. Sieben, J. M.; Duarte, M. M. E.; Mayer, C. E.; *ChemCatChem* **2010**, *2*, 182.
14. Raof, J. B.; Golikan, A. N.; Baghayeri, M.; *J. Solid State Electrochem.* **2010**, *14*, 817.
15. Raof, J. B.; Karimi, M. A.; Hosseini, S. R.; Mangelizadeh, S.; *J. Electroanal. Chem.* **2010**, *638*, 33.
16. El-Deab, M. S.; *Int. J. Electrochem. Sci.* **2009**, *4*, 1329.
17. Zheng, L.; Song, J. F.; *J. Solid State Electrochem.* **2010**, *14*, 43.
18. Wu, B. H.; Hu, D.; Kuang, Y. J.; Liu, B.; Zhang, X. H.; Chen, J. H.; *Angew. Chem., Int. Ed.* **2009**, *48*, 4751.
19. Suffredini, H. B.; Salazar-Banda, G. R.; Avaca, L. A.; *J. Sol-Gel Sci. Technol.* **2009**, *49*, 131.
20. Balasubramanian, A.; Karthikeyan, N.; Giridhar, V. V.; *J. Power Sources* **2008**, *185*, 670.
21. Zhao, H. B.; Li, L.; Yang, J.; Zhang, Y. M.; *Electrochem. Commun.* **2008**, *10*, 1527.
22. Zhang, D.; Ding, Y.; Gao, W.; Chen, H. Y.; Xia, X. H.; *J. Nanosci. Nanotechnol.* **2008**, *8*, 979.
23. Sawyer, D. T.; Roberts, J. L.; *Experimental Electrochemistry for Chemists*, Wiley: New York, 1974.
24. Baumann, J. A.; Salmon, D. J.; Wilson, S. T.; Meyer, T. J.; Hatfield, W. E.; *Inorg. Chem.* **1978**, *17*, 3342.
25. Allinger, N. L.; *J. Am. Chem. Soc.* **1977**, *99*, 8127.
26. Zerner, M. C.; Loew, G. H.; Kirchner, R. F.; Mueller-Westerhoff, U. T.; *J. Am. Chem. Soc.* **1980**, *102*, 589.
27. Formiga, A. L. B.; Nogueira, A. F.; Araki, K.; Toma, H. E.; *New J. Chem.* **2008**, *32*, 1167.
28. Longuet-Higgins, H.; Pople, J. A.; *Proc. Phys. Soc.* **1955**, *68*, 591.
29. Latimer, W. M.; *The oxidation states of the elements and their potentials in aqueous solutions*, Prentice-Hall: Englewood Cliffs, 1952, 2nd ed.
30. Nicholson, R. S.; Shain, I.; *Anal. Chem.* **1964**, *36*, 706.
31. Sundholm, G.; *Acta Chem. Scand.* **1971**, *25*, 3188.
32. Sundholm, G.; *J. Electroanal. Chem.* **1971**, *31*, 265.
33. Nash, T.; *Biochemistry* **1953**, *55*, 416.